Developmental Biology **216,** 282–296 (1999)
Article ID dbio.1999.9487, available online at http://www.idealibrary.com on IDEAL®

Acid Production and Degradation in the Early Chick Embryo

Eric C. Swindell,* Christina Thaller,* Shanthini Sockanathan,† Martin Petkovich,‡ Thomas M. Jessell,† and Gregor Eichele*

**Department of Biochemistry, Baylor College of Medicine, Houston, Texas 77030; ‡Cancer Research Laboratories, Queen's University, Kingston, Ontario K7L 3N6, Canada; and †Howard Hughes Medical Institute and Department of Biochemistry and Molecular Biophysics, Columbia University, New York, New York 10032*

Excess retinoids as well as retinoid deprivation cause abnormal development, suggesting that retinoid homeostasis is critical for proper morphogenesis. RALDH-2 and CYP26, two key enzymes that carry out retinoic acid (RA) synthesis and degradation, respectively, were cloned from the chick and show significant homology with their orthologs in other vertebrates. Expression patterns of *RALDH-2* and *CYP26* genes were determined in the early chick embryo by *in situ* hybridization. During gastrulation and neurulation *RALDH-2* and *CYP26* were expressed in nonoverlapping regions, with *RALDH-2* transcripts localized to the presumptive presomitic and lateral plate mesoderm and *CYP26* mRNA to the presumptive mid- and forebrain. The two domains of expression were separated by an approximately 300-μm-wide gap, encompassing the presumptive hindbrain. In the limb region, a similar spatial segregation of *RALDH-2* and *CYP26* expression was found at stages 14 and 15. Limb region mesoderm expressed *RALDH-2*, whereas the overlying limb ectoderm expressed *CYP26*. RA-synthesizing and -degrading enzymatic activities were measured biochemically in regions expressing *RALDH-2* or *CYP26*. Regions expressing *RALDH-2* generated RA efficiently from precursor retinal but degraded RA only inefficiently. Conversely, tissue expressing *CYP26* efficiently degraded but did not synthesize RA. Localized regions of RA synthesis and degradation mediated by these two enzymes may therefore provide a mechanism to regulate RA homeostasis spatially in vertebrate embryos.

INTRODUCTION

Retinoic acid (RA) is required for the development of vertebrate embryos and also for numerous physiological processes in adults (reviewed in Kastner *et al.*, 1995; Chambon, 1996). One mode of regulation of RA signaling occurs at the transcriptional level. The RA signal is transduced by the retinoic acid receptors (RARs) and retinoid-X receptors (RXRs), two families of transcription factors that control, in a ligand-dependent fashion, the expression of retinoid-responsive genes (reviewed in Mangelsdorf *et al.*, 1994; Mangelsdorf and Evans, 1995). Loss-of-function mutations in the RAR and RXR genes cause specific developmental defects reminiscent of those observed in retinoid-deficient embryos (Kastner *et al.*, 1995; Dickman *et al.*, 1997; Maden *et al.*,1996). Mutations in retinoid responsive genes such as *Hoxa-1* and *Hoxb-1* also cause marked developmental defects (Dupé *et al.*, 1997; Gavalas *et al.*, 1998; Studer *et al.*, 1998).

It has been known since the 1950s that RA is produced from its precursors retinol and retinal through dehydrogenation (Dowling and Wald, 1960). In a rate-limiting first reaction, a retinol dehydrogenase (ROLDH) converts retinol to retinal, which in a second step is converted to RA by a retinal dehydrogenase (RALDH). Several ROLDH and RALDH isozymes that use retinol or retinal as substrates have been isolated (Zgombic-Knight *et al.*, 1995; Chai and Napoli, 1996; Bhat *et al.*, 1995; Duester 1996; Wang *et al.*, 1996; Zhao *et al.*, 1996; Penzes *et al.*, 1997; Napoli, 1996). Regulation of RA-dependent processes may also occur at the level of RA metabolism. Support for this idea comes from studies in which ectopically applied pharmacological

0012-1606/99 $30.00

inhibitors of RA synthesis were shown to have profound effects on the expression of developmental control genes (e.g., Stratford *et al.*, 1996). In addition, recently identified enzymes that synthesize and metabolize RA are expressed in specific patterns in the embryo (Niederrheither *et al.*, 1997; Fujii *et al.*, 1997; Sockanathan *et al.*, 1998; Berggren *et al.*, 1999; and below). For example, in the mouse a class IV alcohol dehydrogenase is first expressed in the mesoderm of the primitive streak as early as E7.5 (Ang and Duester, 1997). The tissue adjacent to the streak also strongly expresses a retinal dehydrogenase, RALDH-2 (Niederreither *et al.*, 1997; Berggren *et al.*, 1999).

RA degradation to oxidative metabolites is initiated by the formation of the polar intermediates 4-hydroxy-retinoic acid and 4-oxo-retinoic acid (Frolik *et al.*, 1979). White *et al.* (1996, 1997), Ray *et al.* (1997) and Fujii *et al.* (1997) have identified a RA-inducible P450 enzyme, termed CYP26, that is a member of a novel cytochrome P450 family. *CYP26* is expressed in a complex pattern throughout mouse development (Fujii *et al.*, 1997). *RALDH-2* and *CYP26* appear to be expressed in complementary expression patterns within the mouse embryo. Restricted regions of RA synthesis and degradation within early embryos might provide a mechanism for regulating RA concentration within these tissues. Such local control of RA concentration could be used to establish distinct cell types or cell fates within an initially uniform set of cells.

The present study compares the patterns of *RALDH-2* and *CYP26* expression in the chick embryo with a focus on the gastrula/neurula-stage chick embryo and on the wing-forming region. We show that the *RALDH-2* and *CYP26* expression patterns predict the spatial distribution of corresponding enzymatic activities. Regions that express *RALDH-2* efficiently generate RA from retinal but exhibit low RA-degrading activity. By contrast, regions expressing *CYP26* effectively degrade but do not synthesize RA. These findings suggest a model in which the expression of previously characterized RA-induced and RA-repressed genes can be understood in terms of the distribution of RA synthetic and metabolic enzymes. More generally, these studies lend additional support to the theory that retinoid metabolism has a critical role in retinoid-dependent developmental processes.

MATERIALS AND METHODS

Isolation of RALDH-2 Fragment

Total RNA was prepared from the lumbar region of stage 26 chick embryos using guanidine hydrochloride and phenol extraction. One microgram of total RNA was used as a template for cDNA synthesis which was initiated from random primers and Superscript reverse transcriptase (Gibco BRL). One-tenth of the cDNA was used for PCR amplification using the following primers: 5′primer, 5′ GGG TCT AGA CA(A/G) AT(C/A/T) AT(C/A/T) CCI TGG AA 3′ 3′primer, 5′ GGG CTC GAG CC(A/G) AA(G/A/T) AT(T/C) TC(T/C) TC(T/C) TT 3′.

After 30 PCR cycles at the annealing temperature of 50°C, the predicted 700-bp fragment was gel purified and subcloned into Bluescript KS. The subclone was then sequenced using standard techniques.

Isolation of a CYP26 Fragment

Total RNA was isolated from stage 4–6 chicken embryos. First-strand cDNA was synthesized using random primers and AMV reverse transcriptase. PCR was carried out using the degenerate oligonucleotides 5′primer, GTTCCGAATCGCCATGIGIATCC, and 3′primer, GTGGTTTCGTGICCTCCAAAIAG. After 40 PCR cycles at the annealing temperature of 55°C, the predicted 360-bp fragment was gel purified and subcloned into pCR-Script (Invitrogen). DNA was then isolated and sequenced.

Isolation of Class I ALDH

Total RNA was isolated from stage 10–15 chicken embryos. First-strand cDNA was synthesized using oligo(dT) primers and AMV reverse transcriptase. PCR was carried out using the oligonucleotides designed from the published chicken class I ALDH sequence (Godbout *et al.*, 1996; Accession No. X58869): 5′primer, ATGAAGAAGCAAGGCTCACC, and 3′primer, GCTAAATTCTGCACATCAAGC. After 35 PCR cycles at the annealing temperature of 68°C, the predicted full-length 1.5-kb fragment was gel purified and subcloned into pCR-Script (Invitrogen). DNA was then isolated and sequenced.

Isolation of Full-Length RALDH-2 and CYP26

The 700-bp *RALDH-2* PCR fragment generated was used to screen 1 million plaques from a Lambda ZAP phage cDNA library prepared from embryonic chick spinal cord. Four different *RALDH-2* clones were isolated and sequenced using standard procedures. The 360-bp *CYP26* PCR fragment generated was used to screen 1 million plaques from a Lambda ZAP stage 18–24 chick limb bud library. Five *CYP26* clones were isolated and sequenced. Sequence analysis was carried out using GCG software.

Transfection

COS cells were stably transfected using Lipofectamine (Gibco BRL) with the vector *pCDNA3* (Invitrogen) containing the entire coding region for *cCYP26* or with vector alone.

Analysis of Metabolites

Transfected COS cells were incubated in D-MEM plus 10% fetal calf serum containing 1 μM RA. Limb bud pieces and embryo pieces were preincubated in D-MEM plus insulin, selenium, and transferrin supplement (Boehringer) for 1 h and then retinal or RA was added to 1 μM. After the noted time points, the medium from these incubations was collected. Retinoids were then isolated and analyzed by HPLC using a Rainin Microsorb MV cyano column eluted with *n*-hexane/isopropanol/methanol/acetic acid (93.5/5/1/0.5) at a flow rate of 0.8 ml/min. Rechromatography of relevant fractions from the cyano column was on a Rainin Microsorb MV

C18 column eluted with methanol/acetonitrile/0.6 M ammonium acetate (64/20/16) at a flow rate of 0.8 ml/min.

In Situ Hybridization

Synthesis of digoxygenin-tagged riboprobes of *CYP26*, *RALDH-2*, and *(ALDH-1)* and whole-mount *in situ* hybridization using these probes were carried out as described by Albrecht *et al.* (1997). Whole-mount *in situ* hybridizations using two riboprobes were carried out as in Albrecht *et al.* (1997) except that after the first color reaction, the embryos were heated for 10 min at 65°C and washed. Thereafter, the embryos were treated with a second antibody directed against the second labeled riboprobe and washed, and a second color reaction was carried out.

RA Treatment of Limb Buds

AG1-X2 ion-exchange beads soaked in RA at a concentration of 100 μg/ml were applied to the anterior margin of HH stage 20 wing buds for the noted times. Embryos were then harvested for short-term limb bud culture or for whole-mount *in situ* hybridization.

RA Treatment of Embryos

Chick embryos were isolated at HH stage 4 and cultured as described in Sundin and Eichele (1992) in the presence of 30 μM RA. After 6 h the embryos were harvested and analyzed by whole-mount *in situ* hybridization.

RESULTS

Isolation of a RALDH-2 cDNA from Chicken

Degenerate primers encoding the amino acids QIIPWN and KEEIFG corresponding to conserved domains in alcohol dehydrogenases (Fig. 1A) were designed from homologous sequences identified in human and rat. These primers were used to generate a 700-bp PCR fragment from cDNA derived from mRNA isolated from the lumbar region of HH stage 26 chicken embryonic spinal cord. A cDNA library prepared from embryonic chick spinal cord was then screened using the PCR fragment as a probe. Four different clones were isolated and found to contain an open reading frame of 1.5 kb. The predicted chicken RALDH-2 protein sequence (Fig. 1A) was 94% identical to the homologous mouse and rat proteins (Wang *et al.*, 1996; Zhao *et al.*, 1996).

Isolation of a CYP26 cDNA from Chicken

mRNA from stage 4–9 chick embryos was reverse transcribed, and degenerate PCR primers encoding amino acid sequences conserved between zebrafish (White *et al.*, 1996) and human CYP26 (White *et al.*, 1997) (Fig. 1B) were used to generate a 360-bp PCR fragment. The PCR fragment was used to isolate a 1.7-kb chicken *CYP26* cDNA from a chick limb bud cDNA library. Figure 1B compares the predicted chicken CYP26 protein sequence with its human, mouse, and zebrafish homologues. Chicken CYP26 (Fig. 1B) and its fish and mammalian homologues are 68 and 80% identical, respectively (White *et al.*, 1996, 1997; Fujii *et al.*, 1997; Ray *et al.*, 1997).

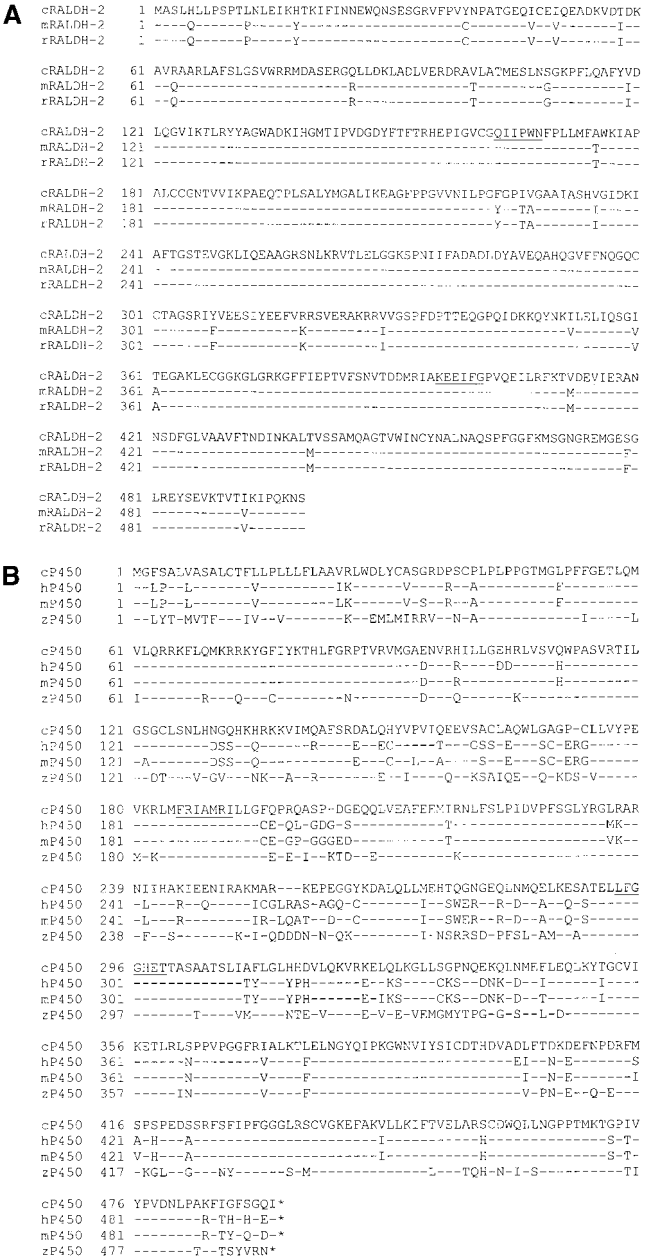

FIG. 1. Comparison of predicted amino acid sequences of RALDH-2 and CYP26 from various vertebrates. The underlined sequences correspond to the primers used for PCR cloning. (A) Amino acid sequence of chicken RALDH-2 compared to mouse and rat homologs. (B) Amino acid sequence of chicken CYP26 compared to human, mouse, and zebrafish homologs.

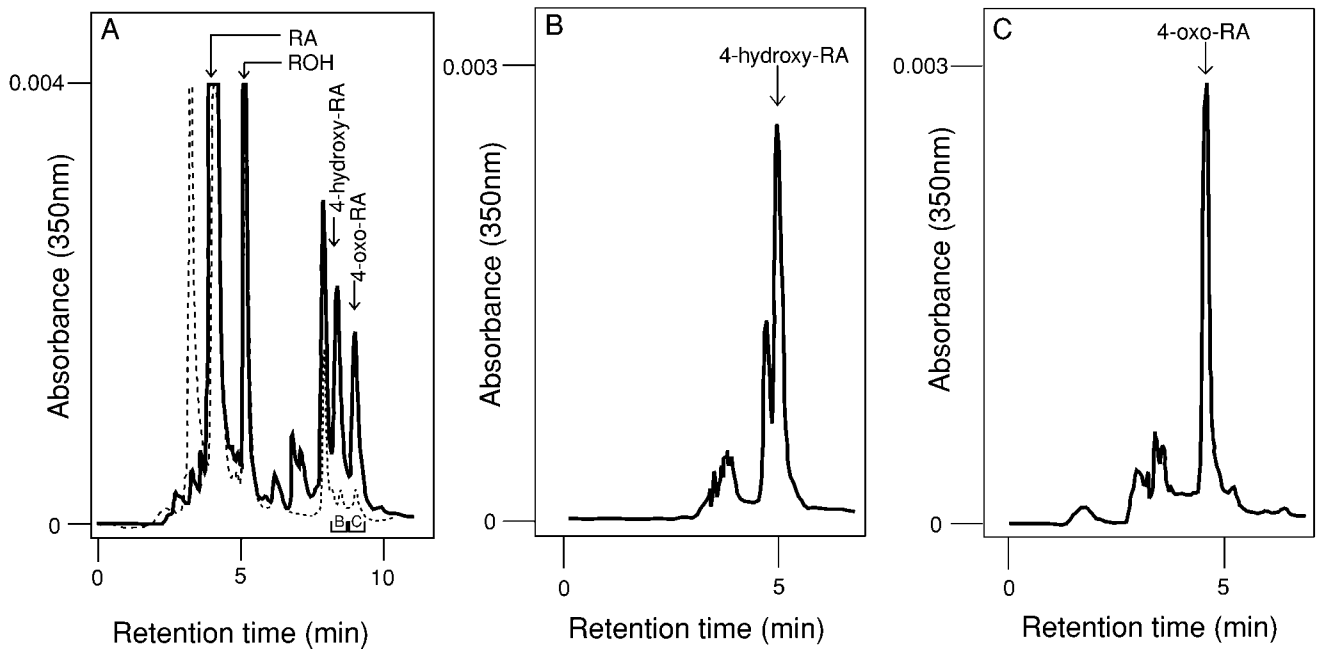

FIG. 2. Characterization of RA metabolites produced by CYP26 transfected into COS cells. (A) The dotted line represents a chromatogram of medium extracted from mock-transfected COS cells and the solid line that from *CYP26*-transfected cells. Fraction pools B and C were rechromatographed resulting in the chromatograms shown in (B) and (C). (B) The major component of pool B coelutes with authentic 4-hydroxy-RA. (C) The major component of pool C coelutes with authentic 4-oxo-RA. Arrows mark the retention time of authentic standards.

Enzymatic Activities of CYP26 in Vitro and in Vivo

The sequences of CYP26 in different species are more divergent than observed with RALDH-2, which prompted us to examine whether the chicken cDNA indeed encoded an enzyme capable of converting RA into its oxidative metabolites. The chicken *CYP26* cDNA was cloned into the eukaryotic expression vector *pCDNA-3* and the resultant plasmid was stably transfected into COS cells. All-*trans*-RA was added at 1 μM to the cells and after 6 h of incubation, metabolites were analyzed by HPLC. Extracts of medium from *CYP26*-transfected and mock-transfected COS cells were separated on a cyanonitrile HPLC column (Fig. 2A). Two peaks that coeluted with authentic 4-hydroxy-RA and 4-oxo-RA were greatly enhanced in the medium of *CPY26*-transfected cells. When the appropriate fractions were collected, pooled (B and C in Fig. 2A), and rechromatographed on a C18 reversed-phase HPLC column, they coeluted with authentic 4-hydroxy-RA (Fig. 2B) and 4-oxo-RA (Fig. 2C). 5,8-Epoxy-RA, a RA metabolite generated by *CYP26*-transfected F9 cells (Fujii *et al.*, 1997), was not detected in our assays. This metabolite would coelute with retinol on the cyanonitrile column (Fig. 2A). When the appropriate fractions were collected, pooled, and reanalyzed on a C18 column, no peak that comigrated with authentic 5,8-epoxy-RA was detected (data not shown). 4-Hydroxy-RA and 4-oxo-RA were found only in COS cell medium; extracts of COS cell pellets did not contain these two metabolites above the level of detection (0.5 to 1 ng), suggesting that these retinoids are secreted. Taken together, our data provide evidence that chicken *CYP26* is a RA-degrading enzyme and is likely to be the avian homologue of the previously identified mouse and human enzymes.

Expression Domains of RALDH-2 and CYP26 Are Nonoverlapping in Gastrula- and Neurula-Stage Chick Embryos

In mouse embryos *RALDH-2* and *CYP26* are expressed in distinct spatial patterns in the early embryo (Niederreither *et al.*, 1997; Fujii *et al.*, 1997). The planar geometry of the early chick embryo is well suited to comparing the expression of these two genes and relating their expression to fate maps of embryonic development. Accordingly, the expression patterns of *RALDH-2* and *CYP26* were determined by whole-mount *in situ* hybridization histochemistry (Figs. 3 and 4). Expression of *RALDH-2* was first detected at HH stage 4 in mesoderm posterior to Hensen's node (Fig. 3A), a region fated to form somitic, intermediate, and lateral plate mesoderm (Garcia-Martinez *et al.*, 1993). At stages 4 and 5, *RALDH-2* is also expressed at low levels in the primitive

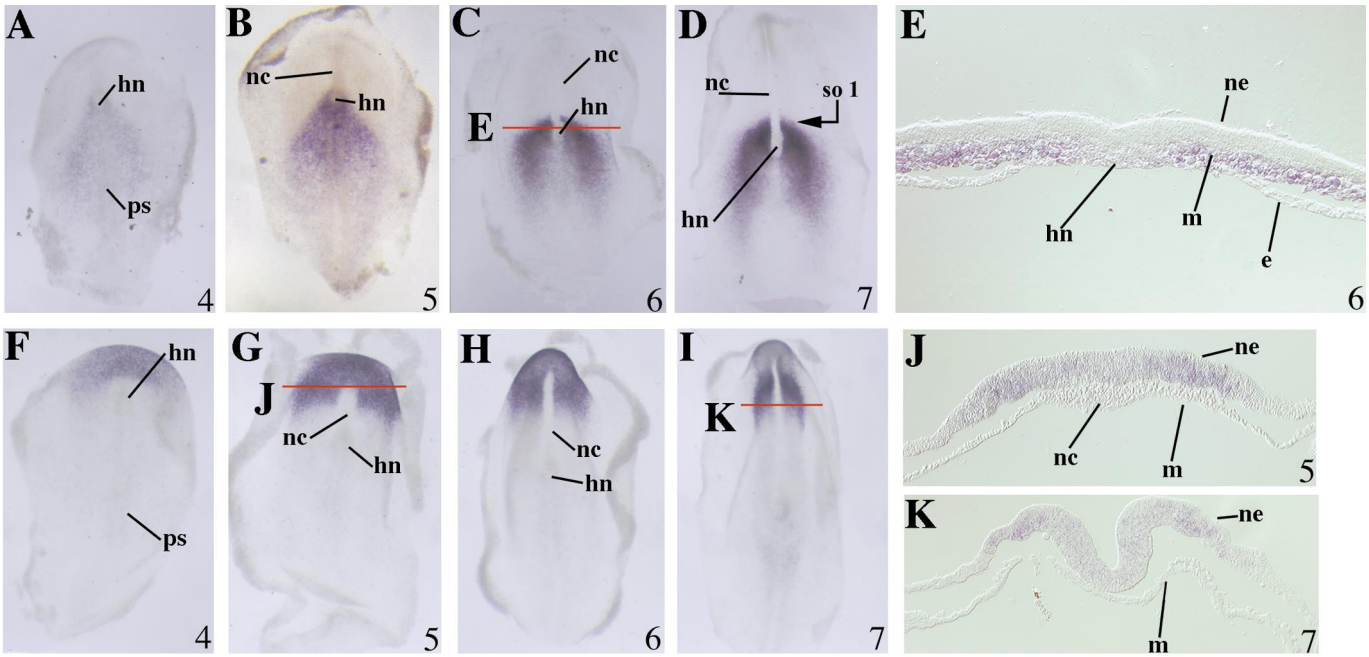

FIG. 3. *cRALDH-2* (A–E) and *cCYP26* (F–K) expression patterns in HH stage 4 to 7 chick embryos revealed by whole-mount *in situ* hybridization. (E, J, and K) Cross sections indicated in (C), (G), and (I) by a red line. Stages are indicated at the bottom. Abbreviations: e, endoderm; hn, Hensen's node; m, mesoderm; nc, notochord; ne, neurectoderm; ps, primitive streak; so, somite.

streak and in cells surrounding the node (Figs. 3A and 3B). At these stages and at all subsequent stages, *RALDH-2* transcripts were largely restricted to mesodermal tissues, except for neural expression in motor neurons (Sockanathan and Jessell, 1998), cells of the roof plate region, and the neural retina. At stage 6, *RALDH-2* expression persisted in mesoderm (Figs. 3C and 3E), but transcripts were absent from the node, the nascent notochord, and the posteriormost region of the embryo. Very high *RALDH-2* expression, however, was detected in nonaxial mesoderm directly surrounding the node (Figs. 3C, 3D, and 3E). At stage 7, mesodermal expression continued and a sharp anterior boundary was seen at the first somite (Fig. 3D). At subsequent stages, *RALDH-2* transcripts were found at very low levels in somites 1–3, at higher levels in somite 4, and at highest levels in more posterior somites and in presomitic mesoderm immediately posterior to the most recently formed somite (Fig. 4A). *RALDH-2* was also expressed in intermediate and lateral plate mesoderm (Figs. 4B and 4E), both in the somatopleure and in the splanchnopleure. Of note, the presumptive wing region (Chaube, 1959; the area between the yellow lines in Fig. 4A) expressed *RALDH-2*. Such expression in the wing field persisted at stage 14 (Fig. 4B), but by stage 15 the level of *RALDH-2* expression was substantially reduced in the nascent wing bud itself (Fig. 4C).

The expression of a class I *ALDH* gene that encodes an enzyme capable of converting retinal into RA has been described in the mouse (Ang and Duester,1997; El Akawi *et al.*, 1994; Bhat *et al.*, 1995). E7.5 mouse embryos expressed this gene in mesoderm of the primitive streak. In the chick, however, this gene was not expressed in embryos of HH stage 4 to 13, a range that encompasses E7.5 of mouse. Figure 5A documents the lack of expression of class I *ALDH* in a stage 5 chick embryo. As previously reported (Godbout *et al.*, 1996) the class I *ALDH* gene was first expressed in the developing chick eye at stage HH14 (Fig. 5B). These data indicate that this class I *ALDH* gene is unlikely to contribute to RA synthesis in the early chick embryo.

CYP26 expression was detected by early stage 4, slightly earlier than *RALDH-2*, in a crescent-shaped domain of ectoderm anterior and lateral to Hensen's node (Fig. 3F) that coincided with the presumptive fore- and midbrain regions (Schoenwolf and Sheard, 1990). At stage 5 to 7, *CYP26* expression persisted in presumptive fore- and midbrain neuroectoderm but the nascent notochord and Hensen's node did not express *CYP26* (Figs. 3G–3K). After stage 7, the level of *CYP26* expression decreased in the anterior part of the embryo. From stage 7 to stage 10, anterior expression became restricted to the dorsal folds of the neural tube and then to a small domain corresponding to rhombomere 2 (Fig. 4F; Vaage, 1969). At stage 10, the only remaining sites of expression were in the hindbrain in rhombomere 2, in the lateral plate endoderm,

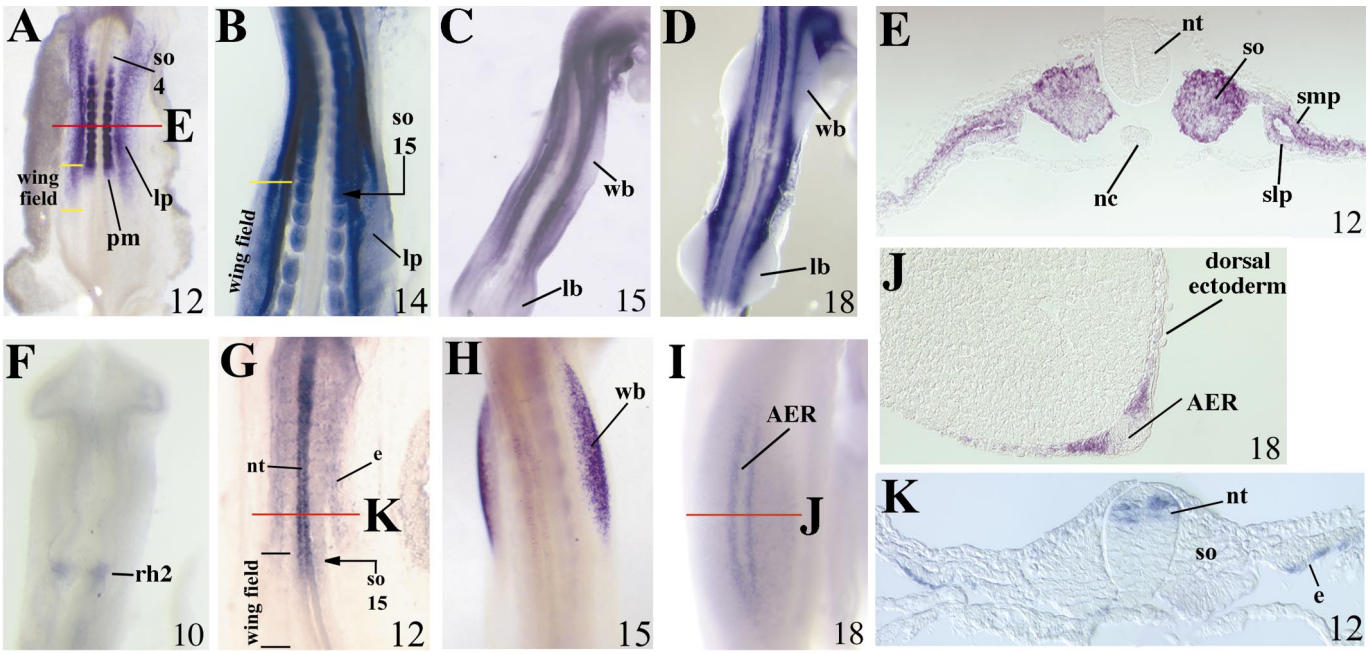

FIG. 4. *cRALDH-2* (A–E) and *cCYP26* (F–K) expression patterns in HH stage 10 to 18 chick embryos revealed by whole-mount *in situ* hybridization. (E, J, and K) Cross sections indicated in (A), (G), and (I) by a red line. The boundaries of the wing field are indicated by yellow (A) or black (G) lines. In (B), the anterior boundary of the wing field is indicated by a yellow line. Stages are indicated at the bottom. Abbreviations: AER, apical ectodermal ridge; lb, leg bud; lp, lateral plate; nt, neural tube; pm, presomitic mesoderm; rh2, rhombomere 2; smp, somatopleure; slp, splanchnopleure; wb, wing bud; for other abbreviations see legend to Fig. 3.

and in the tail bud (data not shown). By stage 11/12, the expression of *CYP26* in rhombomere 2 had disappeared. There was at this stage an initiation of *CYP26* expression in the neural tube (Figs. 4G and 4K). By stage 12, transcripts were seen in the anterior neural tube in a column of five to nine somites in length. As development proceeded, this column was displaced posteriorly and ended in the tail bud region. Figure 4K shows a cross section of a stage 12 chick embryo at somite level 12. *CYP26* expression was confined to dorsal neural tube, close to the roof plate.

Dual-color *in situ* hybridization using *RALDH-2* and *CYP26* probes revealed more precisely a complementarity of expression of these two genes in the early embryo (Fig. 6). *RALDH-2* was expressed in mesoderm posterior to a level defined by the presumptive hindbrain/spinal cord boundary, whereas *CYP26* was expressed anterior to the hindbrain/midbrain boundary. This creates a distinct ~300-μm gap that spans the hindbrain, in which neither gene is expressed.

Expression Domains of RALDH-2 and CYP26 in the Limb Region

Inhibition of retinal dehydrogenases or local application of retinoid receptor antagonists shows that retinoids are required for initial limb bud outgrowth and establishment of the ZPA (Helms *et al.*, 1996; Stratford *et al.*, 1996; Lu *et al.*, 1997). Moreover, Niederreither *et al.* (1999) have recently generated *RALDH-2* mutant mice in which the homozygote embryos die at 10.5 dpc and do not form limb buds. We therefore investigated the patterns of expression of *RALDH-2* and *CYP26* in the limb field and in the nascent limb bud with a focus on the wing region. As noted above, at stage 12 and later, *RALDH-2* was expressed in the somites, in presomitic mesoderm just posterior to the most recently formed somite, and in intermediate and lateral plate mesoderm (Figs. 4A, 4B, and 4E). In the lateral plate, expression took the form of a ribbon that started at the level of the first somite and extended caudally past the axial level defined by the most recently formed somite (Fig. 4A). As additional somites formed, this caudal boundary of *RALDH-2* expression moved progressively more posteriorly and eventually arrived at and then remained in the tail bud. At stage 12 *RALDH-2* mRNA was found in the wing-forming region of the lateral plate (demarcated by the two yellow lines in Fig. 4A). At stage 14 *RALDH-2* mRNA persisted in the wing-forming region of the lateral plate (Fig. 4B), but by stage 15, *RALDH-2* transcript levels were greatly reduced in the nascent wing bud, yet continued to be present at the thoracic level and caudal to the wing region (Fig. 4C). At stage 16, *RALDH-2* expression also decreased

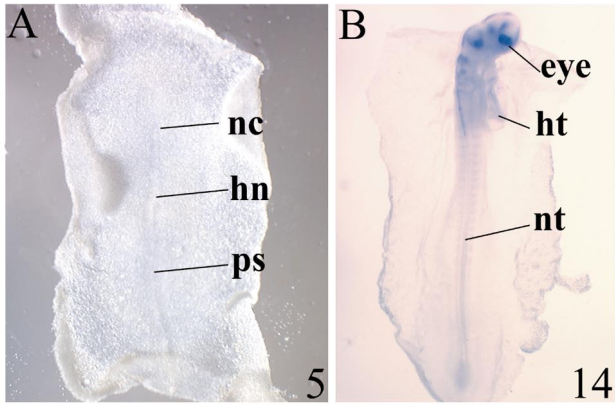

5

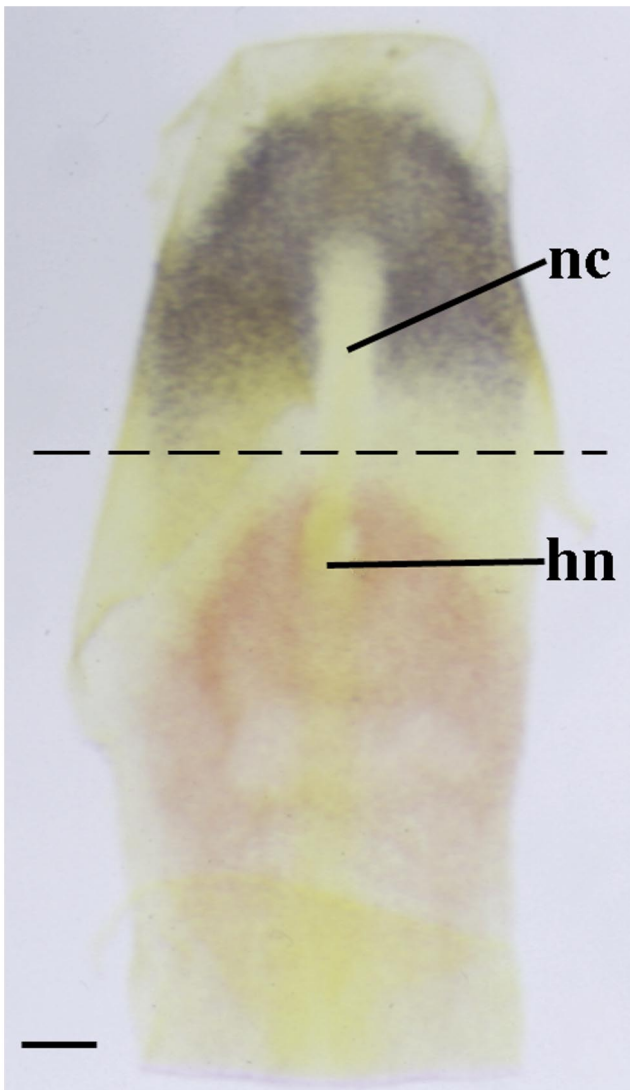

6

FIG. 5. Expression of class I ALDH in HH stage 5 (A) and stage 14 (B) chick embryos. Abbreviations: ht, heart; for other abbreviations see legend to Fig. 3.

in the leg bud region (not shown). Once limb buds had fully formed, they did not express *RALDH-2* except at their base (Fig. 4D).

Stage 11 and 12 embryos expressed *CYP26* in the lateral plate endoderm with a posterior expression boundary just anterior to the most recently formed somite (Figs. 4G and 4K). Such endodermal expression was no longer observed at stage 13 and 14. Around stage 14/15, however, *CYP26* expression initiated in the ectoderm covering the nascent wing bud (Fig. 4H). At stage 16, transcripts were also seen in the ectoderm overlying the leg bud. Expression in limb ectoderm started at stage 14/15, before the formation of the AER (Fig. 4H). Once the AER had developed it bisected the *CYP26* expression domain into a dorsal and ventral stripe (Figs. 4I and 4J). This highly restricted expression domain of *CYP26* began to disappear by stage 26.

The dynamic changes in *RALDH-2* and *CYP26* expression in the wing region and wing bud can be summarized as follows. At stage 12, *RALDH-2* expression is found in the mesoderm of the wing field. In contrast, *CYP26* was not expressed in the wing field at this time. *CYP26,* however, is expressed in endoderm anterior to the wing field. At stage 13, *RALDH-2* expression persisted in the wing-field mesoderm but *CYP26* transcripts were still absent. At stage 14, *RALDH-2* mRNA was still abundant in wing-field mesoderm, and very weak expression of *CYP26* appeared in the overlying ectoderm. At stage 15, when the wing bud begins to develop, the level of *CYP26* expression in ectoderm increased, coincident with a rapid decline in *RALDH-2* expression in mesoderm. Subsequently, *RALDH-2* expression was not detected in the wing bud, whereas *CYP26* continued to be expressed at high levels.

The Relationship between RALDH-2/CYP26 Expression and RA Metabolism

We next investigated whether RA-producing and RA-degrading enzymatic activities reflected the expression patterns of *RALDH-2* and *CYP26.* To test this, stage 5 and 6 embryos were divided into two portions as indicated by a dashed line in Fig. 6. Approximately 20 tissue pieces were incubated for 120 min with either retinal or RA and the metabolites were identified and quantified by HPLC as described for COS cell metabolites. When incubated in retinal in duplicate experiments, the anterior portion of the embryo generated 83 and 32 pg of RA per microgram of DNA, while the posterior portion of the embryo generated 340 and 291 pg of RA per microgram of DNA. When

FIG. 6. Expression of *cCYP26* (purple) and *cRALDH-2* (orange) at stage 6. A dashed line indicates where embryos were divided for enzymatic activity assays (see text). The scale bar represents 300 μm. Abbreviations: see legend to Fig. 3.

incubated with RA in duplicate experiments, the anterior portion of the embryo generated 824 and 221 pg of 4-hydroxy-RA per microgram of DNA, whereas the posterior portion of the embryo generated 148 and 40 pg of 4-hydroxy-RA per microgram of DNA. Although there was variation in the results between the two measurements, the posterior region of the early embryo produced substantially more RA from retinal than the anterior region. Conversely, the anterior region of the same embryos degraded RA more efficiently than the posterior part. These data show that synthesis and degradation of RA reflect the expression domains of *RALDH-2* and *CYP26*.

We next determined whether the pattern of *RALDH-2* expression in the limb region reflected RA synthesis. We dissected stage 18/19 interlimb mesoderm that expressed *RALDH-2* at high levels (Fig. 4D) and for comparison isolated mesoderm from stage 21 wing buds, a tissue that lacks *RALDH-2* transcripts (not shown) and is also devoid of *CYP26* mRNA (Fig. 7A). These tissues were cut into pieces of approximately 350 μm in each dimension and incubated with retinal for 120 min. The amount of RA synthesized was then quantified by HPLC. *RALDH-2*-positive flank tissue produced 183 and 145 pg of RA per microgram of DNA (duplicate measurements), while limb bud mesoderm synthesized only 43 and 30 pg of RA per microgram of DNA. Thus flank tissue is fourfold more efficient in the production of RA than is limb bud mesoderm. These results again show that cells expressing *RALDH-2* efficiently produce RA from retinal.

We then induced *CYP26* in the chick wing bud to determine whether the expression of this gene correlated with increased RA degradation. RA-impregnated beads were implanted at the anterior margin of stage 20 chick wing buds. After 6 h of treatment, a strong induction of *CYP26* was detected in limb bud mesenchyme adjacent to the RA-releasing bead (Fig. 7B). RA-treated limb buds were then divided into anterior and posterior halves and the anterior portion was assayed for induced enzyme activity. This was achieved by incubating fragments of anterior mesenchyme in 1 μM RA for 120 min. We found that the cultured limb bud tissue generated a major peak that coeluted with authentic 4-hydroxy-RA and a minor peak coeluting with authentic 4-oxo-RA (Fig. 7C). Importantly, the RA-treated anterior tissue was approximately 10-fold more efficient in the production of 4-hydroxy-RA than untreated anterior tissue from the contralateral limb (Fig. 7C). Specifically, *CYP26*-positive tissue produced 141 and 78 pg of 4-hydroxy-RA per microgram of DNA (duplicate measurements), while control tissue synthesized 9 and 5 pg of 4-hydroxy-RA per microgram of DNA. Thus the domain of ectopic *CYP26* expression was highly enriched in RA-degrading activity. Of note, under the conditions used, HPLC measurements showed that the bud treated with a RA-releasing bead contained 12% more RA than the contralateral control. This indicates that the amount of RA originating from the bead is much less than that RA provided to tissue by the incubation medium. Therefore, the observed metabolites are predominantly derived from RA that originated from the incubation medium.

Taken together, enzyme activity measurements in limb bud tissue and in early chick embryos demonstrate that regions expressing *RALDH-2* effectively produced RA. Tissues lacking this enzyme, however, did not carry out this reaction efficiently. Similarly, cells expressing *CYP26* degraded RA, whereas those that did not exhibited much less RA degradation. These results support the idea that *CYP26* and *RALDH-2* are major RA-metabolizing enzymes in the chick embryo.

Regulation of Expression of RALDH-2 and CYP26 by RA

CYP26 is inducible by RA in the chick wing bud (see above) as well as in mouse and zebrafish embryos (White *et al.*, 1996; Fujii *et al.*, 1997). Earlier work has shown that several *Hox* genes and *otx-2* are regulated by RA in the embryo. The treatment of chick embryos with RA induced ectopic expression of *Hoxb-1* (Sundin and Eichele, 1992) and repressed *otx*-2 (Bally-Cuif *et al.*, 1995). The RA dose used affected the patterning of hindbrain and craniofacial structures in the chick (Sundin and Eichele, 1992). We therefore examined whether RALDH-2 and CYP26 are also regulated by retinoids *in vivo*. Treatment of stage 4 chick embryos with 30 μM RA in culture for 6 h produced no obvious change on the expression of RALDH-2 (compare Figs. 8A and 8B). This observation suggests that RA does not regulate its own synthesis from retinal. RA treatment, however, resulted in a significant posterolateral extension of the CYP26 domain of expression (compare Figs. 8C and 8D). The sharp posterior boundary of the normal *CYP26* expression domain was lost and cells representing prospective surface ectoderm (Garcia-Martinez *et al.*, 1993) now expressed *CYP26*. The ectopic *CYP26* expression domain, however, did not visibly encroach the *RALDH-2*-expressing presumptive lateral plate. Thus, even in the presence of RA at concentrations capable of having profound effects on development, regions producing and degrading RA remain spatially separate. High concentrations of RA were necessary to affect the expression of *CYP26*, since exposure of embryos to 2 μM RA did not alter its pattern of expression (data not shown).

DISCUSSION

Several enzymes catalyzing RA synthesis and degradation have been identified. An aldehyde dehydrogenase termed RALDH-2 generates RA from its precursor retinal (Wang *et al.*, 1996; Zhao *et al.*, 1996), whereas the P450 enzyme, CYP26, degrades RA to 4-hydroxy RA (White *et al.*, 1996,

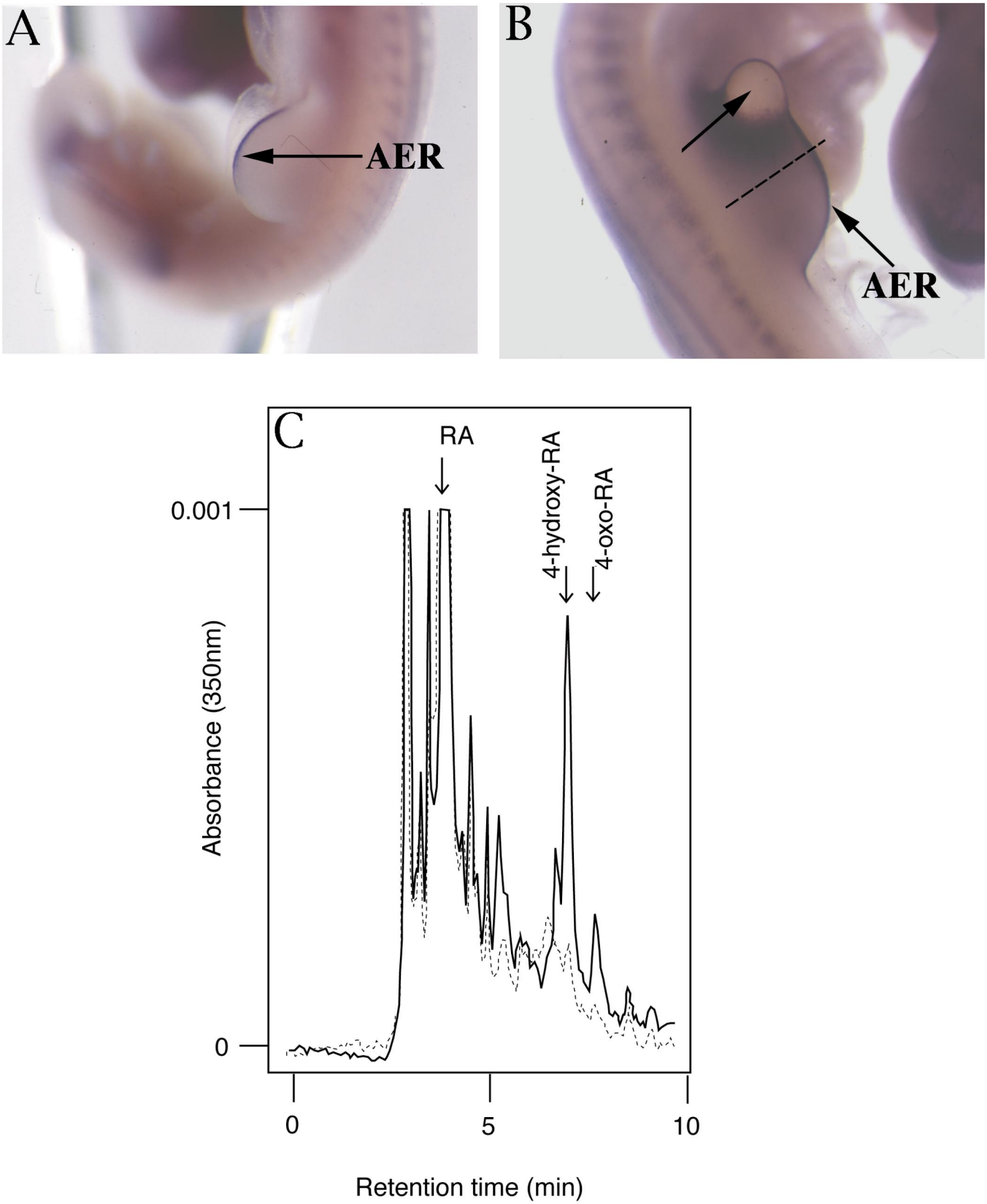

and this study). We have investigated the spatial distribution of these two enzymatic activities in the chick embryo. The patterns of expression of *RALDH-2* and *CYP26* are complementary in the early chick embryo; cells and tissues expressing *RALDH-2* did not express *CYP26* and vice versa. Moreover, tissues that contain *RALDH-2* or *CYP26* mRNA efficiently carry out the corresponding enzymatic conversions. Tissues that do not express *RALDH-2* or *CYP26* metabolize retinal or RA much less efficiently. In the early embryo, in which *CYP26* expression is restricted to the anterior portion of the neural plate, the corresponding enzymatic activity is about six times higher in this tissue than in the presumptive trunk. A similar enrichment in retinal dehydrogenation activity is seen in tissues that express *RALDH-2*. These data suggest that RALDH-2 and CYP26 are major enzymes that catalyze RA production and degradation in the early chick embryo. A class I ALDH gene reported to be expressed in early mouse embryos (Ang and Duester,1997) was not expressed in chick embryos at stages 4 to 13.

Retinol and retinyl esters are the most abundant retinoids in chick embryos and serve as the primary precursors for RA and didehydro-RA (Thaller and Eichele, 1990; Maden *et al.,* 1998). Retinol is converted to retinal by dehydrogenation. The enzyme(s) that catalyzes this reaction has not yet been well studied, but biochemical analyses demonstrate that a class IV alcohol dehydrogenase can convert retinol to retinal (Boleda *et al.,* 1993). This enzyme is expressed in embryonic mesoderm of mouse as early as E7.5 (Ang and Duester, 1997). This implies that embryos can generate retinal that is subsequently dehydrogenated to RA by RALDH-2.

Expression Pattern of RALDH-2 and CYP26 in Mouse and Chick

Niederreither *et al.* (1997) have analyzed *RALDH-2* expression during mouse embryogenesis. Berggren *et al.* (1999) have reported an expression analysis of the RALDH-2 enzyme in chick using an antibody. We note a strong agreement between published expression data and those found here. For example, in presomitic embryos both organisms display strong expression lateral to the primitive streak. Moreover, in mouse and chick, the anterior boundaries of expression are at identical levels and transcripts are restricted to mesoderm. In addition, a similar anterior boundary of retinoic acid production in the chick has been shown by Maden *et al.* (1998) using a RA reporter cell assay. At stages 4 and 5 in the chick embryo, *RALDH-2* is expressed in tissue adjacent to the node as well as in the primitive streak. In the one-somite mouse and chick embryo, *RALDH-2* is not expressed in the node but transcripts are abundant in tissues immediately adjacent to the node and there is little expression in the primitive streak.

The conversion of retinol to RA consists of two steps, a rate-limiting conversion of retinol to retinal and a rapid conversion of retinal to RA. It had previously been suggested that the node region generates RA from retinol (Hogan *et al.,* 1992). Since Hogan *et al.* (1992) did not analyze each step individually, their results are not directly comparable to the studies reported here. Despite this caveat, there is a general agreement between the present study and their data. Hogan *et al.* (1992) report that the node region is a site of RA production. In the present study, we found that cells surrounding the node, but not the node itself, express high levels of *RALDH-2*. Hogan *et al.* (1992) found that tissue in the posterior primitive streak is less efficient in RA production than that in the node region, and the presumptive forebrain tissue is devoid of RA synthesis. Our results show that posterior streak expresses *RALDH-2* only weakly, and forebrain region is devoid of *RALDH-2* transcripts. Using a reporter cell assay, Chen *et al.* (1992) showed that RA synthesis in Hensen's node and surrounding tissue increased threefold from stage 4 to stage 6. This is consistent with the upregulation of *RALDH-2* expression occurring between these stages. In conclusion, our results suggest that the enzymatic activity previously reported (Hogan *et al.,* 1992; Chen *et al.,* 1992) resides in cells surrounding the node and not in the node itself. However, to understand retinoid metabolism in the early embryo more fully, it will also be necessary to identify the enzymes that catalyze the rate-limiting conversion of retinol to retinal and determine their expression patterns.

As in the mouse, older chick embryos show a complex and dynamic *RALDH-2* expression pattern in presomitic mesoderm and the somites. Similar dynamics characterize limb anlagen: stage 12 to 14 wing-field mesoderm expresses *RALDH-2* but in the early stage buds transcripts are noticeably absent only to later reappear in the more developed limbs (data not shown and Niederreither *et al.,* 1997). The high degree of similarity between chick and mouse cDNA

FIG. 7. RA-induced expression of *CYP26* and increased RA degradation colocalize. (A) *CYP26* is expressed in ectoderm dorsally and ventrally of the AER of a stage 20 wing bud. (B) Ectopic application of RA from a bead (arrow) induced ectopic expression of *CYP26* in wing-bud mesenchyme adjacent to the RA bead. (C) The chromatogram, shown as a solid line, is from RA-treated tissue incubated for 120 min in 1 μM RA (B) and displays a distinct peak with a retention time identical to that of authentic 4-hydroxy-RA. By contrast, corresponding tissue from untreated buds incubated with 1 μM RA produced little 4-hydroxy-RA (chromatogram represented by a dotted line).

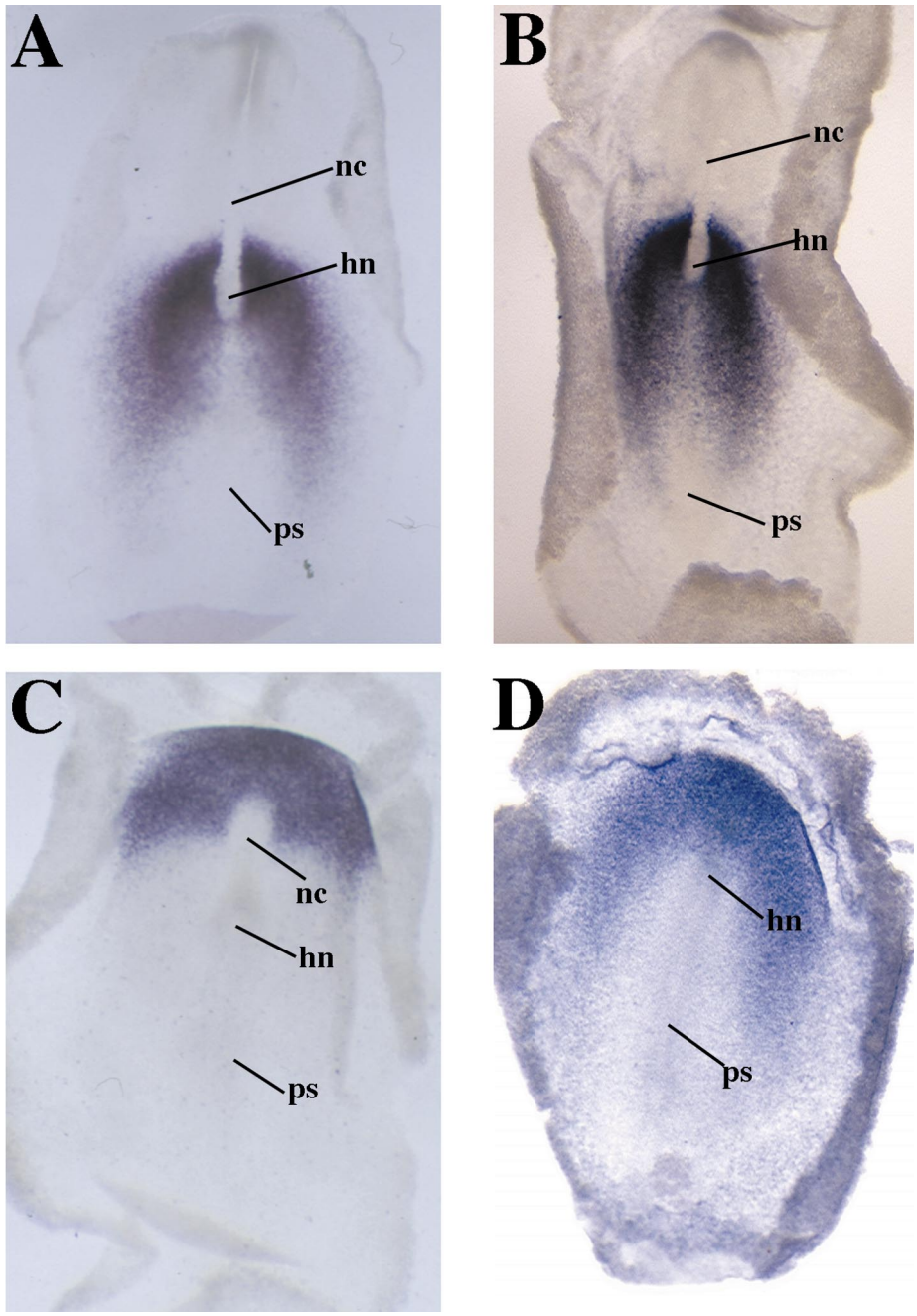

FIG. 8. Effect of RA on expression of *cRALDH-2* and *cCYP26*. (A) Normal expression pattern of *cRALDH-2*. (B) No change of expression pattern of *cRALDH-2* after 6 h of 30 μM RA treatment. (C) Normal expression pattern of *cCYP26*. (D) Alteration of expression pattern of *cCYP26* after 6 h of 30 μM RA treatment. Abbreviations: see legend to Fig. 3.

sequences (94% identity) and expression patterns strongly suggest that these two genes are homologues.

Fujii *et al.* (1997) have carried out an analysis of the expression of the mouse *CYP26* gene. These expression data do not always correlate well with the expression pattern we report here for chick *CYP26*. Although we find that early *CYP26* expression is restricted to the anterior ectoderm, Fujii and co-workers find expression in all three germ layers

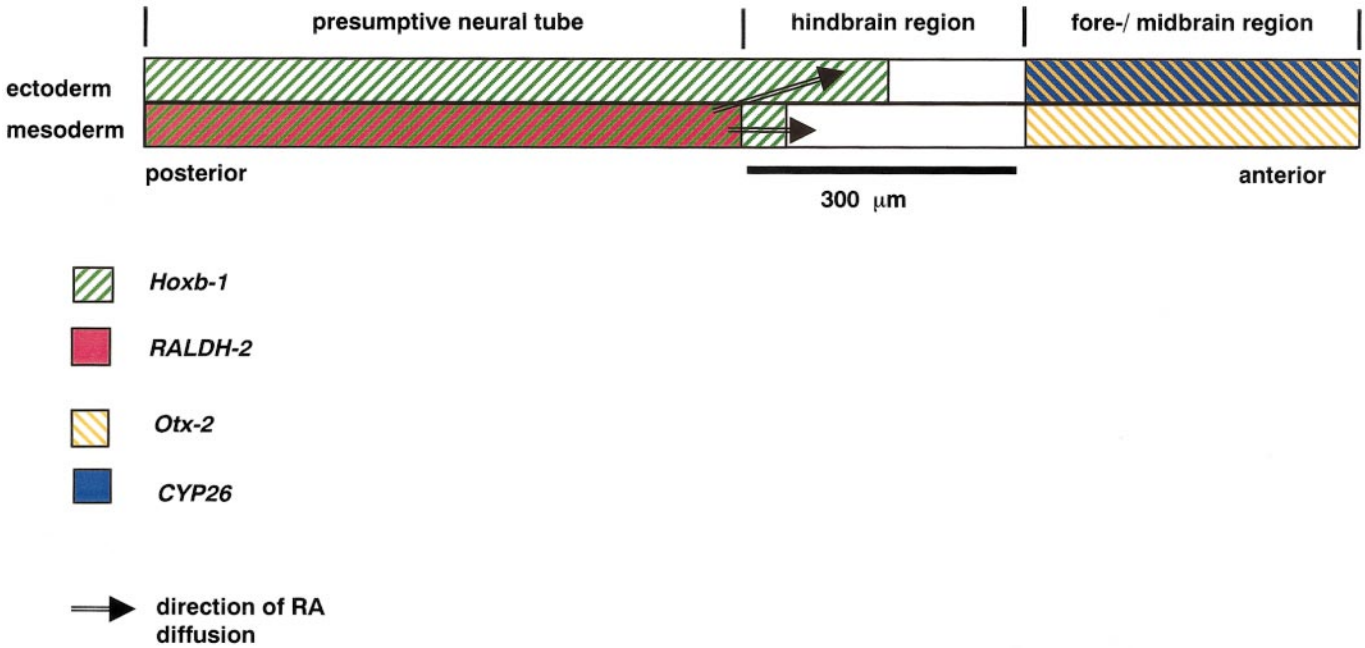

FIG. 9. Model for the contribution of the activities of RALDH-2 and CYP26 to early patterning. RA is produced by RALDH-2 in the posterior mesoderm, turning on selective genes (e.g., *Hoxa-1, Hoxb-1, Hoxb-4*) that require RA for activation. RA diffuses toward the hindbrain, where it turns on genes in ectoderm and mesoderm. RA is then degraded in the anterior region of the embryo by CYP26, allowing the expression of genes that are normally repressed by RA, such as *otx-2*.

as well as in posterior regions of the embryo. At later stages, there is a striking difference in *CYP26* expression in limb buds. At early limb bud stages, we find *CYP26* expression only in the distal limb bud ectoderm, whereas Fujii *et al.* described low levels of expression throughout the limb bud. The chick and mouse data, however, agree with regard to expression of *CYP26* in rhombomere 2 as well as in the domain of expression in the tailbud of later stage embryos. Although the predicted amino acid sequence of chick *CYP26* is 80% identical to that of mouse, the divergence in expression pattern raises the possibility that these genes encode two different but related enzymes. However, all five cDNAs isolated in our library screen represented the chicken *CYP26* gene.

Developmental Relevance of RALDH-2 and CYP26 Expression Patterns

It is well documented that RA regulates certain *Hox* genes in the early embryo. The spatial pattern of expression of *RALDH-2* may be relevant to these findings. *RALDH-2* transcripts are present in mesodermal tissue (Fig. 9) with a sharp anterior border at the hindbrain/spinal cord boundary. We did not detect significant RA-degrading activity in posterior tissue, therefore posterior mesoderm is likely to contain RA. *Hoxb-1,* which is a prototypic RA-regulated *Hox* gene (Marshall *et al.*, 1997; Gavalas *et al.*, 1998), is expressed in this tissue but also in overlying ectoderm/neurectoderm including part of the hindbrain (Fig. 9 and Sundin and Eichele, 1992). For RA to regulate *Hoxb-1* in ectoderm/neurectoderm, RA has to diffuse from its site of synthesis, the mesoderm, into the overlying ectoderm. As indicated in Fig. 9, *Hoxb-1*-positive cells are found in ectoderm as far as 150 μm anterior of the rostral RALDH-2 expression boundary, which suggests that RA might diffuse over such a distance. RA has been shown to diffuse across distances of several hundred micrometers (Eichele and Thaller, 1987). A similar line of reasoning can be applied to *Hoxa-1* and *Hoxb-4,* which are also RA regulated (Dupé *et al.,* 1997; Gould *et al.,* 1998) and are expressed inside but also outside the *RALDH-2* expression domain. Whether RA produced by *RALDH-2* also regulates the expression of *Hox* genes in presumptive neural tube is not clear, but ectopic application of RA to stage 4 embryos increases *Hoxb-1* expression (Sundin and Eichele, 1992), suggesting RA regulation of this gene in this tissue. As an alternative to a diffusion-based mechanism of *Hox* gene regulation, Hogan *et al.* (1992) have discussed a model in which the duration of exposure to an RA source determines *Hox* gene expression.

There is a marked developmentally regulated change in expression of *RALDH-2* in the rostralmost somites. Ini-

tially all 4 anteriormost somites express this gene. By stage 10 (10 somites) and later, however, somites 1 to 3 are virtually devoid of *RALDH-2* mRNA, somite 4 shows some expression, and somite 5 and more posterior somites strongly express this gene. It is interesting to note that in the 10-somite chick, the capacity of somites to induce *Hoxb-4* parallels the level of *RALDH-2* expression in the somites (Itasaki *et al.*, 1996). Specifically, the first 3 somites devoid of *RALDH-2* mRNA lack this capacity, while somite 5 and more posterior somites are very effective in inducing the *Hoxb-4* gene. It has been proposed (Gould *et al.*, 1998) that retinoic acid derived from somites could in part be responsible for regulation of *Hoxb-4* expression, and the differential distribution of *RALDH-2* could be a basis for this process.

In the early chick embryo, *CYP26* expression and hence RA degradation are restricted to the mid- and forebrain region (Fig. 9). Such localized degrading activity may limit the range of RA diffusion to the hindbrain region. Any RA produced by RALDH-2 in posterior mesoderm that diffuses toward the rostral portion of the embryo is likely to be degraded by anteriorly expressed *CYP26*. The juxtaposition of a RA-producing and a RA-degrading domain separated by a gap encompassing the presumptive hindbrain might be expected to give rise to a RA concentration gradient (Crick, 1970). This gradient could be used to specify expression domains of RA-responsive *Hox* genes in the hindbrain region. Because the threshold concentrations of RA required to induce each of these genes differ (Simeone *et al.*, 1990, 1991), a RA gradient spanning the hindbrain region would produce a pattern of overlapping expression domains with different rostral boundaries (reviewed in Hofmann and Eichele, 1994). Whereas several *Hox* genes are RA-inducible in the early embryo, such responsiveness was not observed for *RALDH-2*. In contrast, *CYP26* is RA-inducible, but only at nonphysiological concentrations in the high micromolar range. The nonresponsiveness of the two enzymes that regulate RA homeostasis suggests that their differential expression might form the basis of a retinoid-mediated patterning system.

At high doses, RA is a potent teratogen that adversely affects neural crest cells and hence disrupts craniofacial development (Morriss-Kay and Sokolova, 1996). Thus, the presence of CYP26 in the rostral regions of the embryo could protect against teratogenesis. Along the same lines, upregulation of *CYP26* expression in anterior regions of embryos by exogenous RA might also have a antiteratogenic function. Excess retinoids repress the transcription of *otx-2* (Bally-Cuif *et al.*, 1995), a patterning gene expressed, like *CYP26*, in the presumptive mid- and forebrain ectoderm and mesoderm. Mice lacking *otx-2* fail to undergo the development of cranial structures, indicating that the function of this gene is required for normal head development (Ang *et al.*, 1996; Matsuo *et al.*, 1995). This reasoning suggests that the absence of expression of *CYP26* in rostral tissues would lead to the down-regulation of *otx-2* and a resultant phenotype similar to that of *otx-2* mutant mice.

RA Production and Degradation in the Wing Region

In the lateral plate mesoderm of stage 12/13 embryos, *RALDH-2* is expressed in a column beginning at somite 1 and ending 200–300 μm posterior to somite 15. Thus, *RALDH-2* expression encompasses the presumptive wing mesoderm. *CYP26* is expressed in lateral plate endoderm rostral to somite 15. This arrangement of a RA-synthesizing and a RA-degrading tissue is likely to create a domain of net RA production encompassing the presumptive wing mesoderm, in which retinoid-regulated genes could be activated. An example of such a responsive gene is *Hoxb-8*, which is expressed in wing-bud mesoderm and is RA regulated (Lu *et al.*, 1997). *Hoxb-8* can induce *sonic hedgehog* and *fgf-4*, two factors that mediate limb patterning and outgrowth (see Johnson and Tabin, 1997, for a review). It has also been shown that the blocking of RA signaling at stage 14 prevents the expression of *Hoxb-8*, *sonic hedgehog*, and *fgf-4* (Lu *et al.*, 1997). Whether retinoid signaling regulates the expression of early growth factors, such as *fgf-8* and *fgf-10* (Crossley and Martin, 1995; Ohuchi *et al.*, 1997), in the wing region is not known.

As soon as a limb bud forms, *RALDH-2* is down-regulated, whereas *CYP26* expression is activated in limb bud ectoderm. A consequence of this change in expression would be that limb buds do not generate RA as efficiently as pre-limb-bud mesoderm. This view is consistent with biochemical measurements of RA production that have shown that wing region mesoderm is efficient in producing RA from retinal, but mesenchyme of limb buds is not (Helms *et al.*,1996). The reduction in RA synthesis in the limb bud mesenchyme may account for the observed down-regulation of *Hoxb-8* occurring in this tissue around stage 17/18 (Lu *et al.*, 1997). If RA production persisted in the limb bud at a level found in earlier stages, various patterning genes such as *sonic hedgehog*, *fgf-4*, and *Hoxb-8* would be expressed. Misexpression of limb patterning genes as a result of excess RA would cause a variety of limb patterning defects, such as duplications (Tickle *et al.*, 1982) and truncations (Tamarin *et al.*, 1984), that are observed when exogenous RA is applied to limb buds.

In summary, the intricate spatial and temporal regulation of expression of *RALDH-2* and *CYP26* in the presumptive and definitive limb suggests that RA acts as a developmental switch that regulates the expression of some of the genes required for limb morphogenesis. The fact that *RALDH-2* and *CYP26* are expressed in other tissues, such as the heart (Moss *et al.*, 1998) and the eye, raises the possibility that RA acts in multiple tissues by mechanisms similar to those suggested here to operate in the early embryo and limb bud.

ACKNOWLEDGMENTS

We thank Dr. Sammuel Pfaff for the cloning of a chick *RALDH-2* fragment, Dr. Susan Mackem for supplying a chick limb bud cDNA library, and Dr. Kerby Oberg for comments on the manuscript. This work was supported by the National Institute of Health (G.E., C.T., T.M.J.). T.M.J. is an Investigator of the Howard Hughes Medical Institute.

REFERENCES

Albrecht, U., Eichele, G., Helms, J. A., and Lu, H.-C. (1997). Visualization of gene expression patterns by in situ hybridization. *In* "Molecular and Cellular Methods in Developmental Toxicology" (G. P. Daston, Ed.), pp. 23–48. CRC Press, Boca Raton, FL.

Ang, H. L., and Duester, G. (1997). Initiation of retinoid signaling in primitive streak mouse embryos: Spatiotemporal expression patterns of receptors and metabolic enzymes for ligand synthesis. *Dev. Dyn.* **208,** 536–543.

Ang, S. L., Jin, O., Rhinn, M., Daigle, N., Stevenson, L., and Rossant, J. (1996). A targeted mouse Otx2 mutation leads to severe defects in gastrulation and formation of axial mesoderm and to deletion of rostral brain. *Development* **122,** 243–252.

Bally-Cuif, L., Gulisano, M., Broccoli, V., and Boncinelli, E. (1995). c-otx2 is expressed in two different phases of gastrulation and is sensitive to retinoic acid treatment in chick embryo. *Mech. Dev.* **49,** 49–63.

Berggren, K., McCaffery, P., Drager, U., and Forehand, C. J. (1999). Differential distribution of retinoic acid synthesis in the chicken embryo as determined by immunolocalization of the retinoic acid synthetic enzyme, RALDH-2. *Dev. Biol.* **210,** 288–304.

Bhat, P., Labrecque, J., Boutin, J.-M., Lacroix, A., and Yoshida, A. (1995). Cloning of a cDNA encoding rat aldehyde dehydrogenase with high activity for retinal oxidation. *Gene* **166,** 303–306.

Boleda, M. D., Saubi, N., Farres, J., and Pares, X. (1993). Physiological substrates for rat alcohol dehydrogenase classes: Aldehydes of lipid peroxidation, omega-hydroxy fatty acids, and retinoids. *Arch. Biochem. Biophys.* **307,** 85–90.

Chai, X., and Napoli, J. (1996). Cloning of a rat cDNA encoding retinol dehydrogenase isozyme type III. *Gene* **169,** 219–222.

Chambon, P. (1996). A decade of molecular biology of retinoic acid receptors. *FASEB J.* **10,** 940–954.

Chaube, S. (1959). On axiation and symmetry in the transplanted wing of the chick. *J. Exp. Zool.* **140,** 29–77.

Chen, Y., Huang, L., Russo, A. F., and Solursh, M. (1992). Retinoic acid is enriched in Hensen's node and is developmentally regulated in the early chicken embryo. *Proc. Natl. Acad. Sci. USA* **89,** 10056–10059.

Crick, F. (1970). Diffusion in embryogenesis. *Nature* **5231,** 420–422.

Crossley, P. H., and Martin, G. R. (1995). The mouse Fgf8 gene encodes a family of polypeptides and is expressed in regions that direct outgrowth and patterning in the developing embryo. *Development* **121,** 439–451.

Dickman, E. D., Thaller, C., and Smith, S. M. (1997). Temporally-regulated retinoic acid depletion produces specific neural crest, ocular and nervous system defects. *Development* **124,** 3111–3121.

Dowling, J., and Wald, G. (1960). The biological function of vitamin A acid. *Proc. Natl. Acad. Sci. USA* **46,** 587–608.

Duester, G. (1996). Involvement of alcohol dehydrogenase, short-chain dehydrogenase/reductase, aldehyde dehydrogenase, and cytochrome P450 in the control of retinoid signaling by activation of retinoic acid synthesis. *Biochemistry* **35,** 12221–12227.

Dupé, V., Davenne, M., Brocard, J., Dolle, P., Mark, M., Dierich, A., Chambon, P., and Rijli, F. M. (1997). In vivo functional analysis of the Hoxa-1 3′ retinoic acid response element (3′RARE). *Development* **124,** 399–410.

Eichele, G., and Thaller, C. (1987). Characterization of concentration gradients of a morphogenetically active retinoid in the chick limb bud. *J. Cell Biol.* **105,** 1917–1923.

El Akawi, Z., and Napoli, J. (1994). Rat liver cytosolic retinal dehydrogenase: Comparison of 13-cis-, 9-cis-, and all-trans-retinal as substrates and effects of cellular retinoid-binding proteins and retinoic acid on activity. *Biochemistry* **33,** 1938–1943.

Frolik, C. A., Roberts, A. B., Tavela, T. E., Roller, P. P., Newton, D. L., and Sporn, M. B. (1979). Isolation and identification of 4-hydroxy- and 4-oxoretinoic acid. In vitro metabolites of all-trans-retinoic acid in hamster trachea and liver. *Biochemistry* **18,** 2092–2097.

Fujii, H., Sato, T., Kaneko, S., Gotoh, O., Fulii-Kuriyama, Y., Osawa, K., Kato, S., and Hamada, H. (1997). Metabolic inactivation of retinoic acid by a novel P450 differentially expressed in developing mouse embryo. *EMBO J.* **16,** 4163–4173.

Garcia-Martinez, V., Alvarez, I. S., and Schoenwolf GC. (1993). Locations of the ectodermal and nonectodermal subdivisions of the epiblast at stages 3 and 4 of avian gastrulation and neurulation. *J. Exp. Zool.* **267,** 431–446.

Gavalas, A., Studer, M., Lumsden, A., Rijli, F. M., Krumlauf, R., and Chambon, P. (1998). Hoxa1 and Hoxb1 synergize in patterning the hindbrain, cranial nerves and second pharyngeal arch. *Development* **125,** 1123–1136.

Godbout, R., Packer, M., Poppema, S., and Dabbagh, L. (1996). Localization of cytosolic aldehyde dehydrogenase in the developing chick retina: In situ hybridization and immunohistochemical analyses. *Dev. Dyn.* **205,** 319–331.

Gould, A., Itasaki, N., and Krumlauf, R. (1998). Initiation of rhombomeric Hoxb4 expression requires induction by somites and a retinoid pathway. *Neuron* **21,** 39–51.

Helms, J., Kim, C. H., Thaller, C., and Eichele, G. (1996). Retinoic acid signaling is required during early limb development. *Development* **122,** 1385–1394.

Hofmann, C., and Eichele, G. (1994). Retinoids in development. *In* "The Retinoids" (M. B. Sporn, A. B. Roberts, and D. S. Goodman, Eds.), pp. 387–441. Raven Press, New York.

Hogan, B. L. M., Thaller, C., and Eichele, G. (1992). Evidence that Hensen's node is a site of retinoic acid synthesis. *Nature* **359,** 237–241.

Itasaki, N., Sharpe, J., Morrison, A., and Krumlauf, R. (1996). Reprogramming Hox expression in the vertebrate hindbrain: Influence of paraxial mesoderm and rhombomere transposition. *Neuron* **16,** 487–500.

Johnson, R. L., and Tabin, C. J. (1997). Molecular models for vertebrate limb development. *Cell* **90,** 979–990.

Kastner, P., Mark, M., and Chambon, P. (1995). Nonsteroid nuclear receptors: What are genetic studies telling us about their role in real life? *Cell* **83,** 859–869.

Lu, H.-C., Revelli, J.-P., Goering, L., Thaller, C., and Eichele, G. (1997). Retinoids signaling is required for the establishment of a ZPA and for the expression of *Hoxb-8*, a mediator of ZPA formation. *Development* **124,** 1643–1651.

Maden, M., Gale, E., Kostetskii, I., and Zile, M. (1996). Vitamin A-deficient quail embryos have half a hindbrain and other neural defects. *Curr. Biol.* **6,** 417–426.

Maden, M., Sonneveld, E., van der Saag, P. T., and Gale, E. (1998). The distribution of endogenous retinoic acid in the chick embryo: Implications for developmental mechanisms. *Development* **125,** 4133–4144.

Mangelsdorf, D. J., Umesono, K., and Evans, R. M. (1994). The retinoid receptors. *In* "The Retinoids" (M. B. Sporn, A. B. Roberts, and D. S. Goodman, Eds.), pp. 319–349. Raven Press, New York.

Mangelsdorf, D. J., and Evans, R. M. (1995). The RXR heterodimers and orphan receptors. *Cell* **83,** 841–850.

Marshall, H., Studer, M., Popperl, H., Aparicio, S., Kuroiwa, A., Brenner, S., and Krumlauf, R. (1994). A conserved retinoic acid response element required for early expression of the homeobox gene Hoxb-1. *Nature* **370,** 567–571.

Matsuo, I., Kuratani, S., Kimura, C., Takeda, N., and Aizawa, S. (1995). Mouse Otx2 functions in the formation and patterning of rostral head. *Genes Dev.* **9,** 2646–2658.

Morriss-Kay, G. M., and Sokolova, N. (1996). Embryonic development and pattern formation. *FASEB J.* **10,** 961–968.

Moss, J. B., Xavier-Neto, J., Shapiro, M. D., Nayeem, S. M., McCaffery, P., Drager, U. C., and Rosenthal, N. (1998). Dynamic patterns of retinoic acid synthesis and response in the developing mammalian heart. *Dev. Biol.* **199,** 55–71.

Napoli, J. (1996). Retinoic acid biosynthesis and metabolism. *FASEB J.* **10,** 993–1001.

Niederreither, K., McCaffery, P., Dräger, U. C., Chambon, P., and Dollé, P. (1997). Restricted expression and retinoic acid-induced downregulation of the retinaldehyde dehydrogenase type 2 (RALDH-2) gene during mouse development. *Mech. Dev.* **62,** 67–78.

Niederreither, K., Subbarayan, V., Dolle, P., and Chambon, P. (1999). Embryonic retinoic acid synthesis is essential for early mouse post-implantation development. *Nat. Genet.* **21,** 444–448.

Ohuchi, H., Nakagawa, T., Yamamoto, A., Araga, A., Ohata, T., Ishimaru, Y., Yoshioka, H., Kuwana, T., Nohno, T., Yamasaki, M., Itoh, N., and Noji, S. (1997). The mesenchymal factor, FGF10, initiates and maintains the outgrowth of the chick limb bud through interaction with FGF8, an apical ectodermal factor. *Development* **124,** 2235–2244.

Penzes, P., Wang, X., Sperkova, Z., and Napoli, J. L. (1997). Cloning of a rat cDNA encoding retinal dehydrogenase isozyme type I and its expression in *E. coli*. *Gene* **191,** 167–172.

Ray, W., Bain, G., Yao, M., and Gottlieb, D. I. (1997). CYP26, a novel mammalian cytochrome P450, is induced by retinoic acid and defines a new family. *J. Biol. Chem.* **272,** 18702–18708.

Schoenwolf, G. C., and Sheard, P. (1990). Fate mapping the avian epiblast with focal injections of a fluorescent-histochemical marker: Ectodermal derivatives. *J. Exp. Zool.* **255,** 323–339.

Simeone, A., Acampora, D., Arcioni, L., Andrews, P. W., Boncinelli, E., and Mavilio F. (1990). Sequential activation of HOX2 homeobox genes by retinoic acid in human embryonal carcinoma cells. *Nature* **346,** 763–766.

Simeone, A., Acampora, D., Nigro, V., Faiella, A., D'Esposito, M., Stornaiuolo, A., Mavilio, F., and Boncinelli, E. (1991). Differential regulation by retinoic acid of the homeobox genes of the four HOX loci in human embryonal carcinoma cells. *Mech. Dev.* **33,** 215–227.

Sockanathan, S., and Jessell, T. M. (1998). Motor neuron-derived retinoid signaling specifies the subtype identity of spinal motor neurons. *Cell* **94,** 503–514.

Stratford, T., Horton, C., and Maden, M. (1996). Retinoic acid is required for the initiation of outgrowth in the chick limb bud. *Curr. Biol.* **6,** 1124–1133.

Studer, M., Gavalas, A., Marshall, H., Ariza-McNaughton, L., Rijli, F. M., Chambon, P., and Krumlauf, R. (1998). Genetic interactions between Hoxa1 and Hoxb1 reveal new roles in regulation of early hindbrain patterning. *Development* **125,** 1025–1036.

Sundin, O., and Eichele, G. (1992). An early marker of axial pattern in the chick embryo and its respecification by retinoic acid. *Development* **114,** 841–852.

Tamarin, A., Crawley, A., Lee, J., and Tickle, C. (1984). Analysis of upper beak defects in chicken embryos following with retinoic acid. *J. Embryol. Exp. Morphol.* **84,** 105–123.

Thaller, C., and Eichele, G. (1990). Isolation of 3,4-didehydroretinoic acid, a novel morphogenetic signal in the chick wing bud. *Nature* **345,** 815–819.

Tickle, C., Alberts, B., Wolpert, L., and Lee, J. (1982). Local application of retinoic acid to the limb bond mimics the action of the polarizing region. *Nature* **296,** 564–566.

Vaage, S. (1969). The segmentation of the primitive neural tube in chick embryos (Gallus domesticus). A morphological, histochemical and autoradiographical investigation. *Ergeb. Anat. Entwicklungsgesch.* **41,** 3–87.

Wang, X., Penzes, P., and Napoli, J. L. (1996). Cloning of a cDNA encoding an aldehyde dehydrogenase and its expression in *Escherichia coli*. *J. Biol. Chem.* **271,** 16288–16293.

White, J., Guo, Y.-D., Baetz, K., Beckett-Jones, B., Bonasoro, J., Hsu, K. E., Dilworth, F. J., Jones, G., and Petkovich, M. (1996). Identification of the retinoic acid-inducible all-*trans*-retinoic acid 4 hydroxylase. *J. Biol. Chem.* **271,** 29922–29927.

White, J., Beckett-Jones, B., Guo, Y.-D., Dilworth, F. J., Bonasoro, J., Jones, G., and Petkovich, M. (1997). cDNA cloning of human retinoic acid-metabolizing enzyme (hP450RAI) identifies a novel family of cytochromes P450 (CYP26). *J. Biol. Chem.* **272,** 18538–18541.

Zgombic-Knight, M., Ang, H. L., Foglio, M. H., and Duester, G. (1995). Cloning of the mouse class IV alcohol dehydrogenase (retinol dehydrogenase) cDNA and tissue-specific expression patterns of the murine ADH gene family. *J. Biol. Chem.* **270,** 10868–10877.

Zhao, D., McCaffery, P., Ivins, K. J., Neve, R. L., Hogan, P., Chin, W. W., and Dräger, U. C. (1996). Molecular identification of a major retinoic-acid-synthesizing enzyme, a retinaldehyde-specific dehydrogenase. *Eur. J. Biochem.* **240,** 15–22.

Received for publication April 29, 1999
Revised August 27, 1999
Accepted August 27, 1999